

# Consistent description of electrohydrodynamics in narrow fluidic confinements in the presence of hydrophobic interactions

Jeevanjyoti Chakraborty,<sup>1</sup> Sukumar Pati,<sup>2</sup> S. K. Som,<sup>2</sup> and Suman Chakraborty<sup>1,2,\*</sup>

<sup>1</sup>*Advanced Technology Development Centre, Indian Institute of Technology Kharagpur, Kharagpur-721302, India*

<sup>2</sup>*Mechanical Engineering Department, Indian Institute of Technology Kharagpur, Kharagpur-721302, India*

(Received 18 January 2012; published 11 April 2012)

Electrohydrodynamics in the presence of hydrophobic interactions in narrow confinements is traditionally represented from a continuum viewpoint by a Navier slip-based conceptual paradigm, in which the slip length carries the sole burden of incorporating the effects of substrate wettability on interfacial electromechanics, precluding any explicit dependence of the interfacial potential distribution on the substrate wettability. Here we show that this traditional way of treating electrokinetics-wettability coupling may lead to serious discrepancies in predicting the resultant transport characteristics as manifested through an effective zeta potential. We suggest that an alternative consistent description of the underlying physics through a free-energy-based formalism, in conjunction with considerations of hydrodynamic and electrical property variations consistent with the pertinent phase-field description, may represent the underlying consequences in a more rational manner, as compared to the traditional slip-based model coupled with a two-layer description. Our studies further reveal that the above discrepancies may not occur solely due to the slip-based route of representing the interfacial wettability, but may be additionally attributed to the act of “discretizing” the interfacial phase fraction distribution through an artificial two-layer route.

DOI: [10.1103/PhysRevE.85.046305](https://doi.org/10.1103/PhysRevE.85.046305)

PACS number(s): 47.61.–k

## I. INTRODUCTION

Hydrophobic interactions in narrow confinements have attracted serious research attention over the past few decades [1,2], attributable to the inherent scientific challenges involved, as well as to overwhelming technological implications towards inducing phenomenal reductions in resistive forces against fluidic transport [3]. The physical origin of such interfacial interactions has been scientifically argued for a long time, postulated on the basic notion that hydrophobic effects are likely to trigger the formation of wall-adjacent depleted phases, primarily governed by the fact that the structure of water molecules next to a hydrophobic surface is apparently less ordered than that in the bulk [4–16]. Fundamentally, this has been attributed to the fact that hydrophobic units are not thermodynamically favored to form hydrogen bonds [17]. Irrespective of the details of the generating mechanism of this depleted phase formed near the walls, the latter has been perceived to serve as an effective smoothening blanket, by disallowing the bulk liquid to come in proximate contact with the rough walls.

In the literature, smooth sailing of bulk liquid over an ultrathin cushion of a depleted phase (typically spanning over a length scale of 10 nm) adhering to rough walls, attributable to hydrophobic interactions as described above, has also been conceptualized to give rise to an “apparent slip” phenomenon [18–26], consistent with the physical notion that the liquid apparently slips over the intervening depleted layer, instead of being explicitly slowed down by interference from the wall [27–29]. Such conditions, probed through numerous theoretical and experimental studies [22–89], have been termed as “apparent slip” in the literature, since the no-slip boundary may still remain to be a valid proposition

at the solid boundary (until and unless it falls in the slip flow or rarefied flow regimes of gases). In reality, it is only the apparent inability in resolving the sharp velocity gradients within the ultrathin wall-adjacent depleted layer that prompts an analyzer to extrapolate the velocity profiles obtained in the liquid layer above the low-density blanket, thereby marking an apparent deviation from the no-slip boundary condition at the wall. Despite the underlying simplifications, it has become a common practice to treat hydrodynamics in the presence of hydrophobic interactions through the introduction of a Navier slip coefficient at the confining boundaries in describing the pertinent hydrodynamic boundary condition [90–94].

The implications of hydrophobic interactions and the consequent reductions in fluidic friction, as discussed above, may be far reaching. As an illustration, one may cite the instances of electrohydrodynamic transport in the presence of electrical double layer (EDL) effects. In simple terms, EDL is essentially a charged layer adhering to the solid boundary, typically originated out of involved electrochemical interactions [95,96]. Since typical length scales of the EDL (termed as Debye length in the literature) are likely to be commensurate with the typical length scales of the wall-adjacent depleted layers formed out of hydrophobic effects, their interactions often turn out to be intriguing. Acknowledging this aspect, researchers have reported phenomenal augmentations in the effective electrohydrodynamic transport (characterized by an effective interfacial potential; more formally known as the zeta potential [95]) in the presence of hydrophobic interactions. This has been attributed to an enhanced pumping effect on the solvent molecules in the EDL due to hydrophobic interactions [49,58,66,73,87,97–106].

Consistent with the above conjecture, electrohydrodynamics in the presence of hydrophobic interactions has often been represented as an equivalent electrokinetic transport over slipping surfaces. In an effort towards doing so, however, it needs to be emphasized that it is essential to introduce a slip

\*suman@mech.iitkgp.ernet.in

length that effectively decouples the interfacial hydrodynamics from the intricacies of hydrophobic interactions in the presence of electrokinetic influences. On the basis of this slip length, the standard electrohydrodynamic models can be elegantly closed, disregarding the details of the underlying hydrophobic interactions. The slip length, on the other hand, is routinely estimated from the perceived notion of a given thickness of a depleted interfacial layer that originates out of hydrophobic interactions, by employing a two-layer (a liquid layer on the top of a discrete depleted layer of a given thickness) model [26]. This kind of consideration, despite simplifying the physical paradigm, offers nothing but an abstraction to the physical reality, by attempting to represent the gross artifact of alterations in the interfacial hydrodynamics due to hydrophobic interactions through a discrete two-layer approach, instead of representing the electromechanics and hydrodynamics in the presence of hydrophobic interactions in a coupled environment and thermodynamically consistent manner. As a consequence, the electrohydrodynamics in narrow confinements in the presence of hydrophobic interactions still remain to be poorly understood, especially within the purview of experimentally tractable spatiotemporal scales. This deficit stems from the complexities in describing the underlying interfacial interactions over physical scales that are substantially larger than those addressed in the pertinent molecular scale simulations.

Is the slip-based paradigm of representing the interconnections between hydrophobic interactions and interfacial electromechanics, as routinely adopted in the contemporary literature, physically consistent? Addressing this issue, here we show that the notion of representing interfacial electrohydrodynamics on hydrophobic surfaces by means of an effective slip boundary condition may not remain far from being questionable. In an effort to establish this point, we first outline the traditional approach based on a slip-length-based conceptual paradigm towards estimating an effective zeta potential pertaining to electro-osmotic flow (essentially, a flow triggered by the application of an external electrical field that interacts with free charges within the EDL; for more details, see [95,96]) in a narrow confinement in the presence of hydrophobic interactions. Subsequently, we illustrate the calculation of apparent slip length by extending a two-layer model, which was originally postulated for estimating apparent slip lengths for pressure-driven flows [26], to electro-osmotic transport. This, in turn, acts as a closure to the slip-length-based model (traditional approach), based on a predefined thickness of the interfacial depleted layer, and enables one to calculate the effective zeta potential based on an apparent slip length. Next, as an alternative to this approach, we present a phase-field model that essentially couples the hydrodynamics and electromechanics in the presence of hydrophobic interactions, without being routed through any slip-length-based considerations. Unlike the two-layer model, this model is not based on considerations of predefined discrete layers. Rather, we employ a free-energy minimization approach through the introduction of an order parameter, the distribution of which effectively prescribes the relative phase distributions in a thermodynamically consistent manner, without necessitating a deployment of the paradigm of two discrete layers. Importantly, we use this phase-field parameter to describe the

effective interfacial properties (namely, viscosity and electrical permittivity), instead of preassigning them with discrete values either corresponding to a pure liquid or a pure gaseous phase. This effectively acts as a closure to our electrohydrodynamic model, consistent with the thermomechanics of hydrophobic interactions. In addition, considerations of this model permit us to explicitly relate the contact angle with the resultant electrohydrodynamic transport, which is not possible through a traditional two-layer, or equivalent slip-length-based formalism, with predefined layer thicknesses. More importantly, this allows us to evaluate the interfacial and bulk transport characteristics (such as electrical potential and velocity), without necessitating the employment of a discrete two-layer model. Further, from the resultant bulk transport characteristics, we can compute the effective zeta potential directly, instead of being routed through a traditional slip-length-based approach. Considering the above, on a somewhat nonintuitive note, we demonstrate that there may occur significant discrepancies in the effective zeta potential predictions between the traditional (two-layer) approach and the present formalism, even if the respective layer thicknesses for the discrete two-layer approach are estimated from the same phase-field model considerations as deployed for the present approach. Remarkably, discrepancies in this regard still do remain even if the effective zeta potential is calculated from the bulk transport characteristics consistent with a two-layer description, without necessarily going through the slip-length-based route. We attribute this discrepancy to an apparent inability of the traditional approach in explicitly capturing the interconnection between electrohydrodynamic and hydrophobic interactions, through a thermodynamically consistent postulation of the effective interfacial transport parameters.

The remaining part of this article is organized as follows. In Sec. II A, we first outline the traditional considerations of effective zeta potential predictions based on a predefined slip length, consistent with the reported literature [104]. In Sec. II B, we derive a semianalytical approach for determining the slip length for closing the model outlined in Sec. II A, based on a discrete two-layer model with predefined layer thicknesses, extending the previous works [26] reported in this regard (in the context of pressure-driven flows) to electro-osmotic flows. In Sec. II C, we derive the phase-field-based formalism in detail, towards evaluating the effective zeta potential from the present considerations. In Sec. III, we compare results from the traditional approach (combined slip-length–two-layer approach) with those from the present considerations, and emphasize on the evident discrepancies. We further delineate in this section that discrepancies in the predictions still do remain, even if the effective zeta potential is directly obtained from the two-layer model without going through the slip length route, despite considering the discrete layer thickness to be consistent with the phase-field calculations. In Sec. IV, we draw important conclusions based on our findings reported in this work.

## II. MODEL DESCRIPTION

### A. Effective zeta potential based on Navier slip

In this subsection, as a specific example of electrokinetic transport (without losing generality with regard to the focal

theme of the present investigation), we consider the model problem of electro-osmotic flow (EOF) of a binary electrolyte with symmetric valencies of the cations (+) and the anions (−) through a slit channel of height  $2H$  ( $0 \leq y \leq 2H$ ),  $x$  being the axial direction and  $y$  being the transverse direction. Both the plates have identical homogeneous surface charging conditions. An externally applied electric field  $\mathbf{E}_{\text{app}} \equiv E_{\text{app}} \mathbf{e}_x$  parallel to the channel walls drives the EOF. Because of the fortuitous orthogonality of this particular arrangement, the potential distribution  $\psi^0$  and the charge density  $\rho_e = ez_+c_+^0 + ez_-c_-^0$  due to the EDL in the quiescent state, remain undisturbed by the applied electric field, and thus may be treated separately. The Boltzmann equation governing this quiescent distribution of the ions,  $c_{\pm}^0$ , may be combined with the Poisson equation to obtain the celebrated Poisson-Boltzmann equation for the resolution of the potential distribution  $\psi^0$  screening the surface charge. The solvent hydrodynamics is resolved through the Stokes equation incorporating electrokinetic body force terms; this equation is solved subject to the Navier slip boundary condition at the wall:  $u|_{y=0} = b(\partial u/\partial y)|_{y=0}$  (through a specification of the slip length  $b$ ) and the symmetry condition at the channel center line. The augmentation of flow velocities due to interfacial slip, so obtained, is traditionally expressed in the electrokinetics literature through the introduction of an effective zeta potential,  $\zeta_{\text{eff}}$ , which is expressed in a generic form as

$$\zeta_{\text{eff}} = \zeta \left[ 1 + b \frac{\left( -\frac{\partial \psi}{\partial y} \Big|_{y=0} \right)}{\zeta} \right]. \quad (1)$$

Please note that from this stage, the superscript is dropped with the understanding that the potential distribution established in the quiescent condition remains undisturbed by the fluid flow. The mathematical details behind this overview of expressing the effective zeta potential in terms of the slip length are presented in Appendix A with the standard assumptions to be found in Ref. [107]. For the simplest possible case where the zeta potential is smaller than the thermal voltage [ $\zeta < k_B T/(ez)$ ] so that the Debye-Hückel linearization may be applied, and where the EDL is thin enough so that the channel centre-line ( $y = H$ ) may be considered to be effectively ‘at infinity’, the expression for the potential reduces to  $\psi = \zeta \exp(-\kappa y)$ , where  $\kappa = 1/\lambda = \sqrt{\frac{2n_0 e^2 z^2}{\epsilon k_B T}}$  is the inverse of a characteristic length scale of the EDL (also known as Debye length). Then the effective zeta potential expression, accordingly reads

$$\zeta_{\text{eff}} = \zeta (1 + b\kappa). \quad (2)$$

Other more involved expressions for the effective zeta potential follow Ref. [104] from Eq. (1), based on some relaxations of the aforementioned simplifications.

It is evident from the above description that the determination of effective zeta potential following a slip-length-based conceptual paradigm relies heavily on a correct specification of the slip length  $b$ . In the literature, the latter is commonly accomplished through the introduction of a two-layer model, following the considerations of Tretheway and Meinhart [26] that were originally invoked for pressure-driven flows. In

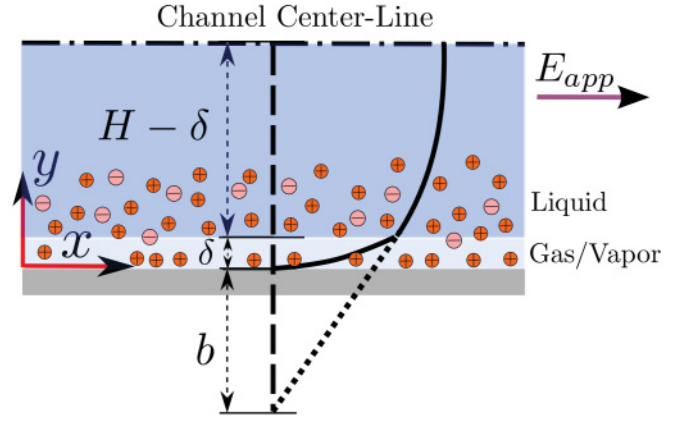


FIG. 1. (Color online) Schematic depiction of a two-layer model, with a discrete depleted (v) layer intervening an outer liquid (l) layer and the wall. The depleted layer is considered to form on the wall as a consequence of hydrophobic interactions [26].

the subsequent subsection, accordingly, we extend those considerations for EOF.

### B. Determination of slip length from a two-layer approach

We schematically represent the paradigm of a two-layer description of interfacial transport as influenced by hydrophobic interactions, considering the formation of a depleted layer blanketing the outer liquid layer from the wall, as depicted in Fig. 1. We consider that the depleted layer is of thickness  $\delta$ , and is characterized by a permittivity of  $\epsilon_v$  and dynamic viscosity of  $\eta_v$ , whereas the outer liquid region (undepleted solvent) is characterized by a permittivity of  $\epsilon_l$  and dynamic viscosity of  $\eta_l$ . The pertinent equations for potential distribution may be mathematically expressed as

$$\epsilon_v \frac{d^2 \psi}{dy^2} = 2c^\infty ez \sinh\left(\frac{ez\psi}{k_B T}\right), \quad 0 \leq y \leq \delta, \quad (3)$$

$$\epsilon_l \frac{d^2 \psi}{dy^2} = 2c^\infty ez \sinh\left(\frac{ez\psi}{k_B T}\right), \quad \delta \leq y \leq H, \quad (4)$$

where  $c^\infty$  is the concentration of the ions in the electroneutral bulk, subject to the boundary conditions

$$\psi(y=0) = \zeta, \quad (5)$$

$$\psi(y \rightarrow \delta^-) = \psi(y \rightarrow \delta^+), \quad (6)$$

$$\epsilon_v \frac{d\psi}{dy}(y \rightarrow \delta^-) = \epsilon_l \frac{d\psi}{dy}(y \rightarrow \delta^+), \quad (7)$$

$$\frac{d\psi}{dy}(y=H) = 0. \quad (8)$$

The corresponding equations governing the flow velocity read

$$\eta_v \frac{\partial^2 u}{\partial y^2} = \rho_e E_{\text{app}}, \quad 0 \leq y \leq \delta, \quad (9)$$

$$\eta_l \frac{\partial^2 u}{\partial y^2} = \rho_e E_{\text{app}}, \quad \delta \leq y \leq H, \quad (10)$$

subject to the boundary conditions

$$u(y=0) = 0, \quad (11)$$

$$u(y \rightarrow \delta^-) = u(y \rightarrow \delta^+), \quad (12)$$

$$\eta_v \frac{du}{dy}(y \rightarrow \delta^-) = \eta_l \frac{du}{dy}(y \rightarrow \delta^+), \quad (13)$$

$$\frac{du}{dy}(y = H) = 0. \quad (14)$$

Following the approach of Tretheway and Meinhardt [26], one may estimate the slip length ( $b$ ) by using the relation

$$u|_{y=\delta} = (b + \delta) \left. \frac{\partial u}{\partial y} \right|_{y=\delta}. \quad (15)$$

Having obtained the slip length, the steps outlined in Sec. II A may be invoked for the estimation of the effective zeta potential to represent the hydrophobicity mediated electro-osmotic flow augmentation. In the following discussions, we refer to this approach as the slip-based route. It needs to be noted here that this approach is conceptually not new, and has only been summarized here, with a vision to form a basis of comparison with respect to the alternative strategy as discussed subsequently.

The slip-based route, as outlined above, is inherently constrained by the fact that it grossly simplifies the entire physics of hydrophobic interactions through the prescription of a particular slip length that may only be a partially effective abstraction of the underlying thermophysical details. Moreover, the two-layer approach invoked for estimating the slip length itself effectively discretizes the depleted and the bulk phases, without considering the issues of interfacial property variations across the phase-separating region. In other words, the discrete two-layer model does not exhibit any sensitive and explicit dependence of the property (for example, permittivity and viscosity) variations based on the relative distributions of the two phases (depleted and bulk) being separated across the interfacial layer.

Conceptually, the above deficits may be potentially overcome by introducing a phase-field-based approach in which thermodynamically consistent variation of a phase field parameter essentially takes the burden of not only ascertaining the relative distributions of the phases being separated from free-energy-based considerations (rather than specifying a discrete depleted layer thickness on an *ad hoc* basis), but also ascertains the viscosity and permittivity variations across the interfacial layer in accordance with the relative phase fraction distribution. This obviates the necessity of not only the employment of a slip-based approach, but also the consideration of an artificially postulated two-layer formalism that is routinely invoked in the literature to represent the hydrodynamic consequences of hydrophobic interactions. Additionally, this formalism is able to explicitly capture the effect of the substrate wettability (through an explicit dependence on the contact angle) on the electrohydrodynamic transport within the interfacial layer, instead of being routed through synthetically posed soft model parameters.

In the Sec. II C, we describe this phase-field approach for obtaining the effective zeta potential (henceforth referred to as the “present approach”) in an elaborate manner.

### C. Phase-field-based formalism

The primary motivation behind the use of the phase-field model stems from the understanding that the depletion of solvent molecules in the vicinity of a hydrophobic substrate

is basically a phase-separation phenomenon of a single component fluid into its vapor and liquid phases. Thus, the fluid is considered to be a binary mixture of liquid and vapor phases, which, under the influence of hydrophobic interactions, undergoes a demixing process. In order to track the spatial variation of the composition of this binary mixture, an order parameter variable  $\phi = (n_1 - n_2)/(n_1 + n_2)$  is introduced, where  $n_i$  are the number densities of the two separating phases. It is this order parameter variable that takes the sole burden of capturing the transition of electrical and hydrodynamic properties across the interfacial layer, and thus precludes the necessity of considering two distinct layers with discrete properties. In the present study,  $\phi = -1$  represents the bulk liquid phase and  $\phi = 1$  represents the vapor phase, with an averaged location of a smeared boundary between the two being considered corresponding to  $\phi = 0$ .

It is extremely important to note here that the ensuing phase-field model development follows closely that of Ref. [25] together with the underlying restrictions and assumptions. Of particular significance is the artifice of calculating the equilibrium order parameter variation taking no cognizance of the flow characteristics. The primary justification for such an artifice is the assumption of a weak influence of flow on the equilibrium distribution of the separating phases. Drawing an analogy, the phase-field model of the hydrophobicity mediated depletion is similar in spirit to the modeling of the electro-osmotic flow where the equilibrium charge distribution is considered practically undisturbed by the flow driven by the relatively weak applied electric field.

In the phase-field model invoked for the present electrohydrodynamic considerations, description of the demixing thermodynamics is achieved through a free-energy functional which represents the excess Ginzburg-Landau free energy for a binary mixture, and is given by [108]:

$$\Delta\Omega(\phi) = \int_0^\infty \left[ \frac{k}{2} \left( \frac{d\phi}{dy} \right)^2 + \Delta\omega(\phi) \right] dy + \Psi_S, \quad (16)$$

where  $\Delta\omega(\phi) = \omega(\phi) - \omega(\phi_0) - (\phi - \phi_0)(\partial\omega/\partial\phi)_{\phi_0}$  is the free energy required to produce a unit volume of uniform fluid of composition  $\phi$  from a large reservoir at composition  $\phi_0$ ,  $0.5k(d\phi/dy)^2$  is the penalty for the presence of the interfacial gradient, and  $\Psi_S$  is the surface energy that takes into account the interactions between the substrate and the fluid. Motivated by the requirement that there should be two minima in the free energy because the two phases (liquid + vapor) must coexist, a double-well shaped form of  $\Delta\omega$  is adopted following Refs. [29,109]:

$$\Delta\omega = \frac{B}{4} \left( \phi - \sqrt{\frac{A}{B}} \right)^2 \left( \phi + \sqrt{\frac{A}{B}} \right)^2, \quad (17)$$

where  $A$  and  $B$  are two positive constants such that  $A, B \sim k_B T_C$  with  $T_C$  being the critical temperature for the liquid-vapor coexistence [29]. This form of  $\Delta\omega$  clearly shows the double-well shape with minima at  $\phi_{\text{eq}} = +\sqrt{A/B}$ ,  $-\sqrt{A/B}$ , representing, respectively, the bulk order parameter values for the vapor and the liquid.

It may be noted in the above context that the requirement of having two minima is an extremely fundamental one in demixing phenomenon irrespective of the geometry and the nature of

the problem that is being addressed because it is a necessity for the existence of two stable phases resulting from the demixing process. The simplest realization (in mathematical terms) of such a requirement is through the double-well potential used. The fundamental genesis of the double-well potential is from the van der Waals equation of state. It has been a preferred choice for phase-separation problems including liquid-vapor phase separation. Indeed, there are numerous examples in the literature where this simple double-well potential has been used [110–120]. From a very general perspective, other forms of the potential (to take into account a generic demixing phenomenon) do exist in the literature; a comprehensive discussion of such forms is present in Chen’s review [121]. The ubiquity and usefulness of the double-well potential can be gauged from the fact that even in this comprehensive discussion [121], the alternative forms are presented as variations on the double-well potential. For instance, there is the double-obstacle potential form which imposes, for the sake of easier numerical implementation, the demixed stable phase values of the order parameter just outside the interfacial region instead of the more physically intuitive smooth transition that is an important characteristic of the double-well potential form. Another one is the sinusoidal potential form which may be useful for spatially periodic manifestations of demixing zones. Interestingly, such a sinusoidal form may be adapted to a case such as ours by considering a suitably selected “period.” It might be interesting to note that we had previously worked with a subtly different mathematical treatment as presented by Andrienko *et al.* [25] which involves a different potential form. However, in the course of development of our work, we settled on the current formulation with the particular choice of the double-well potential because of two reasons: First, unlike Andrienko *et al.* [25], we are not investigating the influence of the temperature, and, as discussed in Chen’s review [121], it is necessary to incorporate the temperature dependence in the potential form only when the overall problem so demands. Second, the double-well potential is more easily tractable numerically and even affords an immediate physical insight by being amenable to a preliminary perturbation analysis without actually implementing the numerics; this preliminary perturbation analysis will be discussed following the establishment of the governing equation for the variation of the order parameter variable. *However, most importantly, the two forms of the potential do not give different results.* The reason is simple: Our mathematical treatment is such that once the order parameter profile is established the details of the phase-field formulation become inconsequential to the transport problem addressed. As such, so long as different forms and formulations result in essentially similar order parameter profiles (as they do indeed for the two mentioned forms), the minor quantitative variations have practically no influence on the final results, and certainly not on the conclusions deduced from the trends of these final results.

In our subsequent analysis, we adopt the principle of free-energy minimization towards obtaining an equilibrium order parameter profile, which we then apply for solving the fluid flow equations. In the following discussion, we explain the genesis of this important consideration of using the equilibrium order parameter profile in the case of the nonequilibrium electrokinetic transport phenomenon. In fact, the question about

the validity of such a consideration might also arise in the case of simple shear-driven (plane Couette) flow or pressure-driven (plane-Poiseuille) flow. As such, we explain, first, the scenario for which our use of the equilibrium order parameter profile (brought about through the minimization of the free-energy functional) is valid for such a simple flow situation. We next discuss the specific case of the electrokinetic transport relevant to our work. This discussion incorporates an interesting analogy between the use of equilibrium profiles of the order parameter profile and the profile of the ion number densities.

In order to avoid any confusion with the nomenclature associated with the concepts to be discussed, we state foremost that the term “nonequilibrium phenomena” might refer to both stationary and nonstationary (i.e., where the system evolves with time) ones (please see, for instance, de Groot and Mazur [122]). A steady-state fluid flow situation where the velocity field is independent of time, and is only a function of the spatial coordinates (in a Eulerian description) is a simple example of stationary nonequilibrium phenomenon. In contrast, a fluid flow situation comprising a phase-separating mixture where the interfaces evolve with time (thus, in turn, affecting the velocity profiles to change with time, too) is an example of a nonstationary nonequilibrium phenomenon.

For the sake of concreteness, let us consider the simple case of shear-driven (plane-Couette) flow taking place within a slit channel with hydrophobic wall substrate. Such a flow situation had been analyzed by Andrienko *et al.* [25]. They too had utilized the equilibrium order parameter profile (with no flow taking place) to predict slip lengths under the shear drive providing a full-fledged theoretical justification (based on principles of nonequilibrium thermodynamics) for such an artifice. We shall not repeat those steps here (please see the Appendix of their paper for the exact details). Rather, we shall try to highlight the key concepts on which their justification is based. The first key concept is that the substrates are perfectly homogeneous and the walls are perfectly parallel to each other resulting in a perfectly unidirectional flow. Thus, the flow profile at any cross section is exactly identical to the flow profile at any other cross section. The second key concept is that under stationary conditions, the interfacial diffusional flux between the two phases (vapor and liquid) is, by definition, zero. This is extremely important to recognize because any interfacial flux will necessarily imply evolution of the interfaces with time and, as such, a nonstationary flow situation (precluded by the initial assumption). These concepts immediately ensure that whatever order parameter profile is established in the equilibrium (no-flow) situation is also maintained even when the flow is taking place. Graphically speaking, it might be said that the equilibrium order parameter profile gets swept along with the flow but fixing our attention to a cross section (with fixed Eulerian coordinates) the order parameter profile (and hence the interfacial structure) does not appear to change. It is extremely important to understand that this situation is mainly a consequence of the fortunate orthogonality of the flow direction with the direction along which the variation of the equilibrium order parameter is established. It is interesting to note what happens, as a consequence of the above discussions) to the various terms of the Cahn-Hilliard equation (which would strictly model this nonequilibrium flow situation, albeit with unnecessary

numerical difficulties):

$$\frac{\partial \phi}{\partial t} + \vec{u} \cdot \nabla \phi = \nabla \cdot (M \nabla \mu), \quad (18)$$

where  $\phi$  is the order parameter variable,  $\vec{u}$  is the velocity field,  $M$  is the mobility, and  $\mu$  is the chemical potential. The first term is immediately recognized to vanish as a consequence of the stationary assumption. The second term is also zero because  $\vec{u} = \{u, 0, 0\}$  and  $\phi = f(y)$  where  $y$  is the coordinate axis perpendicular to the wall such that  $\nabla \phi$  is also a function solely of  $y$ , thus resulting in the inner product being zero. Finally, the interfacial flux is represented as

$$\vec{j} = -\nabla \mu. \quad (19)$$

The condition of zero interfacial flux (associated with the stationary state condition) implies  $\nabla \mu = 0$  such that the Cahn-Hilliard equation is identically satisfied by the equilibrium profile assumption. Indeed, it was only to take into account the evolution of the interfaces with time that Cahn and Hilliard originally proposed their celebrated equation as a generalization of the equilibrium order parameter description [109,111].

The scenario just described synchronizes well with the electrokinetic transport problem addressed in the present work. It is a well-established practice in theoretical modeling of electro-osmotic transport of an ionic solution through a slit channel to utilize the equilibrium profile of the ionic number density in the momentum equation for the description of the velocity profile, with the implicit understanding that the flow itself does not disturb the equilibrium profile, mathematically described by the Poisson-Boltzmann equation. The physical justification behind this practice is exactly identical to the justification presented previously in the case of the order parameter profile. The application of the electric field actuates the flow. However, the electric field itself does not change the equilibrium profile of the ionic number density. Again the key factors behind this are the stationary state condition, the perfect homogeneity of the substrate (this time from an electrochemical perspective), and the fortunate orthogonality between the direction of establishment of the equilibrium profile of the ions and the flow direction. These, of course, ensure that the unidirectionality of the flow itself is maintained.

It thus important to recognize that the flow does not *effectively* disturb either the equilibrium profile of the order parameter (and hence the interfacial fluid structure) nor does it *effectively* disturb the equilibrium profile of the ionic number density. Furthermore, the only link between the interfacial structure (described through the order parameter profile) and the electrochemistry is through the permittivity of the fluid. For the present case the permittivity is assumed to be independent from the influences of the electric field, and is solely a material property of the fluid. This ensures that there is only a one-way coupling (albeit indirect) between the interfacial structure and the electrochemical description. This allows the interfacial structure to be described first using the order parameter variable through the route of minimization of the free-energy functional independent from any electrochemical influences (as done in the present work) and the electrochemical description to be subsequently established through the Poisson-Boltzmann equation. The aforementioned one-way

coupling is due to the fact that the Poisson-Boltzmann equation needs the information of the permittivity of the fluid.

In view of the above discussion, the route, adopted in the present work, of using the equilibrium order parameter profile (independent from any influences of the flow or even electrochemical influences) based on the minimization of the free-energy functional may be accepted as physically justified for the sake of addressing the electro-osmotic flow taking place in the slit channel with perfectly homogeneous walls.

Proceeding further forward, we may now note that a minimization of the free-energy functional Eq. (16) results in the Euler-Lagrange equation:

$$\frac{d\Delta\omega}{d\phi} - \frac{d}{dy} \left[ \frac{k}{2} \frac{d}{d\phi'} \left\{ \left( \frac{d\phi}{dy} \right)^2 \right\} \right] = 0, \quad (20)$$

so that

$$\Delta\omega = \frac{k}{2} \left( \frac{d\phi}{dy} \right)^2 + \text{constant}, \quad (21)$$

together with the boundary condition at  $y = 0$ ,

$$\frac{d\Psi_S}{d\phi} - \frac{d}{d\phi'} \left( \frac{k}{2} \phi'^2 \right) = 0,$$

implicating

$$\frac{d\Psi_S}{d\phi} - k \frac{d\phi}{dy} \Big|_{y=0} = 0. \quad (22)$$

In the bulk,  $\Delta\omega = d\phi/dy = 0$ , so that from Eq. (21), we get

$$\Delta\omega = \frac{k}{2} \left( \frac{d\phi}{dy} \right)^2, \quad \text{or} \quad (23)$$

$$\frac{d\phi}{dy} = \pm \sqrt{\frac{2\Delta\omega}{k}}.$$

The profile for the order parameter may be obtained from Eqs. (20) and (22). Importantly, the use of the boundary condition given by Eq. (22) requires an explicit specification of  $\Psi_S$  in terms of the short-range surface field and the surface enhancement parameters [123]. However, in order to render the interfacial electrohydrodynamics to be explicitly sensitive to the substrate wettability, it may be imperative to link the interfacial order parameter variations with the contact angle  $\theta_w$ .

In an effort to explicitly link the interfacial electrohydrodynamics with the substrate wettability through a phase-field route, it is worthwhile to note that the equilibrium free energy is nothing but the minimum value of the functional Eq. (16). Thus,

$$\gamma = \Omega_{\min} = \Psi_S + \int_{y_1}^{y_2} \frac{k}{2} \left( \frac{d\phi}{dy} \right)^2 2dy. \quad (24)$$

Changing the variable of integration from  $y$  to  $\phi$ , we get

$$\begin{aligned} \gamma &= \Psi_S + \int_{\phi_s}^{\phi_0} \left( \frac{d\phi}{dy} \right)^2 \frac{dy}{d\phi} d\phi \\ &= \Psi_S + \int_{\phi_s}^{\phi_0} \sqrt{2k\Delta\omega} d\phi. \end{aligned} \quad (25)$$

With this general scheme in place, the surface free energies of the solid-vapor, solid-liquid, and liquid-vapor for a droplet-solid-vapor system may be written as

$$\gamma_{sv} = \Psi_S + \int_{\beta}^{\phi_S} \sqrt{2k\Delta\omega} d\phi, \quad (26a)$$

$$\gamma_{sl} = \Psi_S + \int_{\phi_S}^{-\beta} \sqrt{2k\Delta\omega} d\phi, \quad (26b)$$

$$\gamma_{lv} = \int_{\beta}^{-\beta} \sqrt{2k\Delta\omega} d\phi. \quad (26c)$$

It is important to note the absence of any solid surface contribution to Eq. (26c). Now, following [124], use of the celebrated Young's equation for the contact angle, as given by  $\cos \theta_w = (\gamma_{sv} - \gamma_{sl})/\gamma_{lv}$ , results in

$$\cos \theta_w = \frac{\phi_S^3 - 3\beta^2\phi_S}{2\beta^3}, \quad (27)$$

where  $\beta = \sqrt{A/B}$ . Thus, the boundary condition at the wall,  $y = 0$ , becomes

$$\phi|_{y=0} = \phi_S = f(\theta_w; \beta), \quad (28)$$

where  $f$  is a function of the contact angle  $\theta_w$  and the parameter  $\beta$ .

The profile of the phase-field variable may be obtained from Eq. (20), which, together with the form of  $\Delta\omega$  adopted in Eq. (17), becomes

$$\frac{d^2\phi}{d\bar{y}^2} - \frac{BH^2}{k}(\phi^2 - \beta^2)\phi = 0, \quad (29)$$

where  $\bar{y} = \frac{y}{H}$ . The pertinent boundary conditions are Eq. (28) and the bulk condition:

$$\phi(\bar{y} = 1) = -\beta. \quad (30)$$

It is to be noted that  $k \sim B\xi^2$  where  $\xi$  is a measure of the interfacial thickness (up to a multiplicative constant) so that the coefficient of the nonlinear term in Eq. (29) is  $C = H^2/\xi^2 \gg 1$ . Alternatively, using  $\varepsilon = 1/C \ll 1$ , Eq. (29) is immediately recast in the form of a singular perturbation problem, with the interfacial layer where the depletion occurs acting as the "boundary layer." A preliminary perturbation analysis immediately evinces two facts: First, the outer solution up to  $O(1)$  is a constant profile  $\phi^o = -\beta$  matching the bulk boundary condition; second, generalized stretching transformations  $y \rightarrow \xi\varepsilon^r$  and  $\phi \rightarrow \Phi\varepsilon^s$  followed by the requirement of obtaining distinguished limits [125] as  $\varepsilon \rightarrow 0$  result in the values  $r = 1/2$  and  $s = 0$  so that the interfacial thickness is of the order of  $\sqrt{\varepsilon}$ . However, the inner equation provides no respite from the nonlinearity, and recourse has to be taken to numerical methods for the solution of Eq. (29). Importantly, however, the information of the solution nature obtained from the perturbation analysis (albeit incomplete) guides such numerical solution. Here, we solve Eq. (29) using a control-volume-based finite difference approach, together with a continuation technique [126] to resolve the difficulties associated with  $\varepsilon \ll 1$  or, equivalently  $C \gg 1$ .

With this information on the variation of the solvent number density in terms of the phase-field parameter  $\phi$ , one may now describe the interfacial variations of viscosity and permittivity

as explicit functions of  $\phi$ , which acts as the necessary closure to the present mathematical formalism. In an effort to represent this feature in a mathematically simplistic manner, yet without sacrificing the essential physics, we essentially adopt here linearized functional dependences, as described below:

$$\epsilon = \epsilon_v \frac{1 + \phi}{2} + \epsilon_l \frac{1 - \phi}{2}, \quad (31)$$

$$\eta = \eta_v \frac{1 + \phi}{2} + \eta_l \frac{1 - \phi}{2}. \quad (32)$$

It may be important to mention in this context that the dynamic viscosity and the electrical permittivity of the solvent are both material properties. These come about as an upscaled continuum level manifestation of the mechanical and electrical interactions among the solvent molecules. As such, it is intuitive to expect that these properties will be inherently linked to the actual number of molecules present. Again, within the phase-field formalism presented in our work, the order parameter variable is a representation of the relative distribution of the number density of the liquid and "depleted liquid" phases of the same fluid molecules. Therefore, it is physically plausible that both the dynamic viscosity and the electrical permittivity of the fluid should be proportional to the variation of this order parameter variable. In particular, the linear variation ensures that the nature of the variations in the number density (captured by the order parameter variable) is reflected exactly in the variation of these two physicochemical properties of the fluid. There is perhaps no similarly cogent physical justification for any choice other than the linear variation one that has been considered in our work, and, similarly, in previous works (please see, for instance, the works by Andrienko *et al.* [25], Ding and Spelt [127], Borgia and Bestehorn [128], and Park *et al.* [129]). Indeed, any nonlinear dependence of the variation of the dynamic viscosity and the electrical permittivity on the order parameter variation would necessarily imply the imposition of *ad hoc* variations aberrant with the underlying variations in the fluid. It is also worthwhile to note that the particular form of the permittivity variation adopted here is qualitatively similar to the sigmoidal variation with spatial coordinate as *assumed* by Le and Zhang [130]. However, brought about through the route of a simple linear dependence on the phase-field parameter representing the solvent number density, the permittivity variation (as considered here) is far more physically justified than the assumed form in Ref. [130], and is perhaps a more natural reflection of the variation of the number density of the solvent molecules in the depletion zone. Moreover, compared to Ref. [130], the variation of  $\varepsilon$ , in the current formulation, has an explicit dependence on the degree of substrate wettability (through the specification of  $\theta_w$ ), which distinguishes the present approach from the approaches described in Ref. [130]. Interestingly, however, it is important to mention that both these variations may be found to be practically superimposed on each other through suitable matching of ancillary parameters. Notably, such decrements in permittivity values with solvent depletion in the proximity of hydrophobic substrates have been extensively discussed by Mishchuk [131,132]. Finally, we wish to stress that the focus of our work is to capture the effect of smooth variation in physicochemical properties brought on by structural changes

in the fluid due to hydrophobic effects on electro-osmotic flow augmentation. It is important to appreciate that the simple yet physically justified linear variation described through Eqs. (31) and (32) does indeed realize this objective without any unnecessary complications, and captures the essential physics to the extent that the conclusions become significant.

With the variations of  $\epsilon$  and  $\eta$  in place, the potential variation  $\psi(y)$ , and, subsequently, the flow field  $u(y)$  may be determined without the necessity of invoking an “artificial” air and/or gas layer to model for representing the depletion zone. The corresponding closing system of governing differential equations reads

$$\frac{\partial}{\partial \bar{y}} \left[ \bar{\epsilon}(\phi) \frac{\partial \bar{\psi}}{\partial \bar{y}} \right] = K^2 \sinh(\bar{\psi}), \quad (33)$$

where  $K = H/\lambda_l$  with  $\lambda_l = \sqrt{\epsilon_l k_B T / (2c_0 e^2 z^2)}$  being the Debye length based on the liquid permittivity value  $\epsilon_l$ ,  $\bar{\epsilon} = \epsilon/\epsilon_l$ ,  $\bar{\psi} = ez\psi/(k_B T)$ ,  $\bar{y} = y/H$ , and

$$0 = \frac{\partial}{\partial \bar{y}} \left[ \bar{\eta}(\phi) \frac{\partial \bar{u}}{\partial \bar{y}} \right] - \frac{K^2}{\bar{\zeta}} \sinh(\bar{\psi}), \quad (34)$$

where  $\bar{\eta} = \eta/\eta_l$  with  $\eta_l$  the dynamic viscosity of the liquid,  $\bar{u} = u/u_{HS}$  with  $u_{HS} = -\epsilon_l \zeta E_{app}/\eta_l$  being the Helmholtz-Smoluchowski velocity scale, and  $\bar{\zeta} = ez\zeta/(k_B T)$ . These equations are subject to the boundary conditions

$$\bar{\psi} = \bar{\zeta} \quad \text{and} \quad \bar{u} = 0 \quad \text{at} \quad \bar{y} = 0, \quad (35a)$$

$$\frac{\partial \bar{\psi}}{\partial \bar{y}} = 0 \quad \text{and} \quad \frac{\partial \bar{u}}{\partial \bar{y}} = 0 \quad \text{at} \quad \bar{y} = 1, \quad (35b)$$

the latter reflecting the symmetry at the channel center line. We numerically solve Eqs. (33) and (34) using a control volume-based finite difference [133]. Finally, we determine the effective zeta potential considering the bulk phase velocity variations, consistent with the definition delineated earlier.

### III. RESULTS AND DISCUSSIONS

#### A. Variation in $\phi$ and depleted layer “thickness”

One important objective of the subsequent part of this article is to compare the predictions from the slip-based approach with the present approach, both from a qualitative as well as quantitative perspective. However, in an effort towards doing so, one needs to make an estimate of the slip length for the slip-based model, which may be achieved by invoking a two-layer approach as described earlier. Having said that, one must recognize here that a consistent description of the depleted layer thickness  $\delta$  (instead of invoking artificial preassigned values for the same), in turn, is essential for establishing a physically appropriate basis of comparison between the two models. This basis of comparison, in essence, may be realized by calculating an effective depleted layer thickness from the phase-field model itself, so as to ensure a thermodynamically consistent consideration. Rationally, this may work as the best possible basis for the comparison between the two models by eliminating any potential errors that might be accrued through an *ad hoc* plug-in of the depleted layer thickness.

In the present subsection, we illustrate a typical variation in the parameter  $\phi$  with distance from the wall ( $y$ ), as function of the contact angle at the wall ( $\theta_w$ ). In the context of the objective of our work, this serves two purposes. For the slip-based model, the distribution of  $\phi$  helps in determining an equivalent thickness of the depleted layer in a sense that one may consider the distance from the wall where  $\phi$  becomes zero to be equal to  $\delta$ . On the other hand, in the context of the present approach, the distribution of  $\phi$  helps to assess the viscosity and permittivity variations of the fluid across the interfacial layer, thereby serving as a closure to the underlying mathematical description.

In an effort to illustrate typical wall-normal variations in  $\phi$ , we choose  $\beta = 1$  (see [29,87]) and  $C = (H/\xi)^2 = 100$ . As shown in Fig. 2, the value of  $\phi$  decreases from the surface value ( $\phi_S$ ) dictated by the wall boundary condition corresponding to  $\theta_w = 140^\circ$  (chosen for the sole purpose of illustration), and smoothly merges into the bulk undepleted liquid value ( $\phi = -1$ ). The variation of the surface value  $\phi_S$  with the contact angle  $\theta_w$  is shown in the inset of Fig. 2. Higher values of  $\phi_S$  corresponding to higher values of the contact angle indicate that the surface value is closer to the “bulk” vapor value consistent with stronger hydrophobic effects of the wall. Based on the interfacial description established as above, we subsequently attempt to answer the question “To what extent are discrepancies (if any) between predictions from the slip-based approach and the present approach manifested in spite of a compatible basis of their interfacial description?”

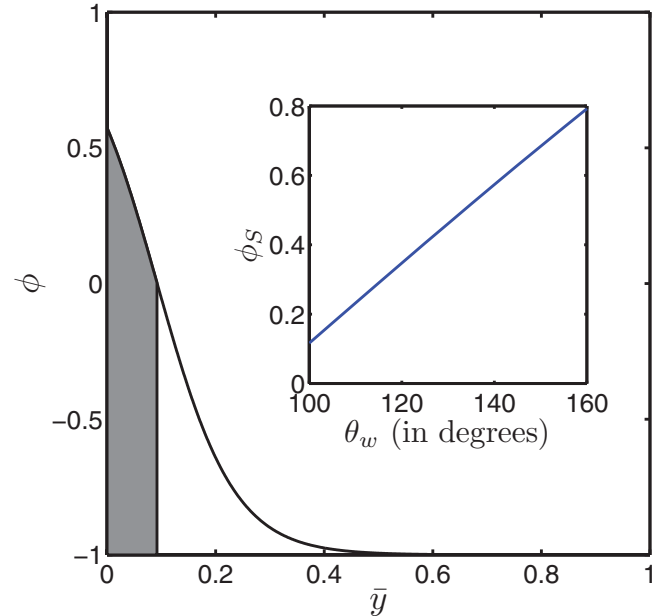


FIG. 2. (Color online) Variation of the phase-field variable  $\phi$  in the direction transverse to the wall for  $\theta_w = 140^\circ$  and  $C = (H/\lambda_l)^2 = 100$ . The shaded region represents the discrete interfacial vapor region of the two-layer model such that  $0 \leq \bar{y} \leq \bar{\delta}$  with  $\phi(\bar{y} = \bar{\delta}) = 0$ . The inset shows the variation of the wall boundary condition for  $\phi$  corresponding to increasing values of the contact angle representing higher degrees of hydrophobicity of the substrate.

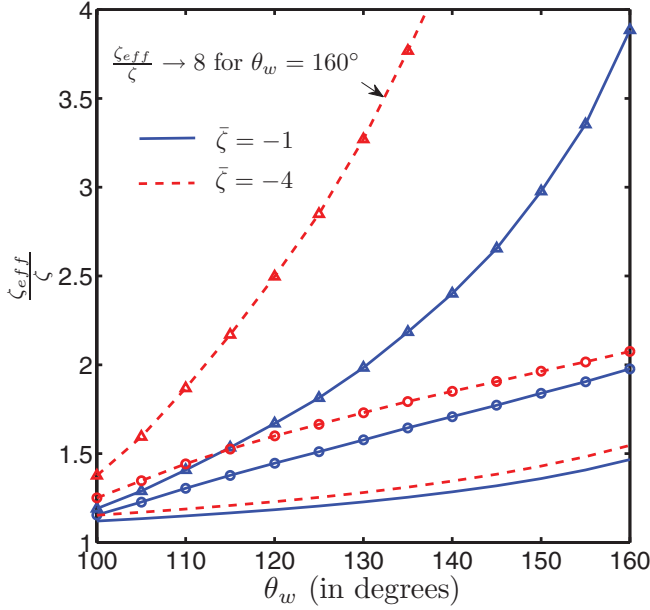


FIG. 3. (Color online) Variation of the effective normalized zeta potential with the contact angle for  $\bar{\zeta} = -1$  (represented by solid lines) and  $\bar{\zeta} = -4$  (represented by dashed lines) with  $K = 5$ ,  $\epsilon_{ratio} = 0.8$ , and  $\eta_{ratio} = 1/3$ . Results from the present approach are depicted by the plots without markers. For the two-layer approach, the slip-length-based route is depicted by  $\Delta$  while the direct bulk-velocity analogy route for the calculation of the effective zeta potential is depicted by  $\circ$ .

**B. Effective  $\bar{\zeta}$ : Variation with  $\theta_w$**

**1. Comparison between predictions from the slip-based model and the present approach**

With a common basis of comparison established by considering the depleted layer thickness to be predicted by the phase-field model, we first present a comparative assessment of the predictions from the slip-based model and the present model. As a basis of comparison, we consider the effective zeta potential as an appropriate transport parameter, for its inherent potentiality in representing the combined electrohydrodynamic consequences. Notably, for the slip-based approach, we determine the effective zeta potential following the slip-length route outlined in Secs. II A and II B. For the present approach, however, we determine the effective zeta potential directly on the basis of the bulk velocity, by drawing an analogy with the Helmholtz-Smoluchowski velocity form, as delineated earlier. For plotting representative characteristics depicting the above comparison, we fix up values of  $\epsilon_{ratio} = \epsilon_v/\epsilon_l$  and  $\eta_{ratio} = \eta_v/\eta_l$  at 0.8 (following Ref. [130]) and 1/3 (following Ref. [25]), respectively. Notably, we have studied the corresponding variations with several other plausible values of these ratios, with a mere effect of modifying the quantitative scenario while retaining similar qualitative trends. We do not show those additional results here for the sake of brevity.

*a. Influence of  $\zeta$ .* Figure 3 shows the variation of  $\zeta_{eff}/\zeta$  with the contact angle  $\theta_w$ , corresponding to the two different values of  $\bar{\zeta} = -1, -4$ , where  $\bar{\zeta}$  implicates a dimensionless zeta potential, and a value of  $K = 5$ , where  $K$  implicates channel half height to Debye length ratio. A general trend

that is evident from this figure is that  $\zeta_{eff}/\zeta$  increases with increase in  $\theta_w$ , irrespective of the mathematical model adopted. This trend is in accordance with an intuitive expectation that with higher degrees of hydrophobicity, more effective electrokinetic pumping of fluid takes place within the interfacial layer, which, by viscous interactions, pulls the bulk fluid more effectively. However, by comparing the trends obtained through the slip-based approach (lines with triangular markers) and the present approach (lines without markers), significant differences between the corresponding predictions may be noticed. While the slip-based approach results in predictions of giant amplifications in the effective zeta potential with increments in the contact angle at the wall, the corresponding increments exhibited by the present approach are somewhat more subtle. This may be attributed to the fact that by considering an effective slip at the wall, the slip length in the slip-based approach tends to propagate the effect of augmented transport at the wall to the bulk in a somewhat exaggerated fashion, as compared to an implicit transmission of the corresponding effect through a continuously varying fluid viscosity across the interfacial layer in accordance with the present approach. Interestingly, the slip-based approach exhibits a more prominent variation of the effective zeta potential with the zeta potential itself, as compared to the present approach. This may be attributed to the fact that the entire fluid in the slip-based approach is assigned the value of the bulk liquid permittivity, which is somewhat larger than the vapor phase permittivity (we have verified this by studying cases in which the differences between the permittivity values of the two phases are higher, which evidently lead to more severe disparities in the predictions from the two models, with regard to variations following the zeta potential). On the other hand, in the present model, there occurs a distribution of the permittivity across the interfacial layer with diminished permittivity values close to the wall, resulting in the prediction of a more “ineffective” propagation of the message of electrochemical perturbation to the bulk. This relatively ineffective response to the electrochemical interactions at the wall, however, appears to be more practical, in a sense that there is a low-density (and also low-permittivity) phase distribution across the interfacial layer that tends to diminish the net number density of the ionic species in the wall-adjacent layers to a large extent. This, in turn, is manifested through only a relatively modest electrokinetic pumping in the bulk, as compared to the extent of electrokinetic pumping that is predicted by the slip-based approach.

*b. Influence of  $K = H/\lambda_D$ .* Figure 4 shows the variation of  $\zeta_{eff}/\zeta$  with the contact angle  $\theta_w$  corresponding to the two different values of  $K = 5, 25$  and a value of  $\bar{\zeta} = -1$ . Again, by comparing the trends obtained through the slip-based approach (lines with triangular markers) and the present approach (lines without markers), significant discrepancies between the corresponding predictions may be noticed, which may be attributed to the reasons mentioned earlier. These discrepancies appear to be more severe with relative thinning of the EDL. The thinner the EDL, the higher the velocity gradient appears to be across the same. Considerations of this towards alteration of the near-wall flow characteristics are explicitly built in with the Navier slip-based boundary condition that is consistent with the slip-based model, which effectively

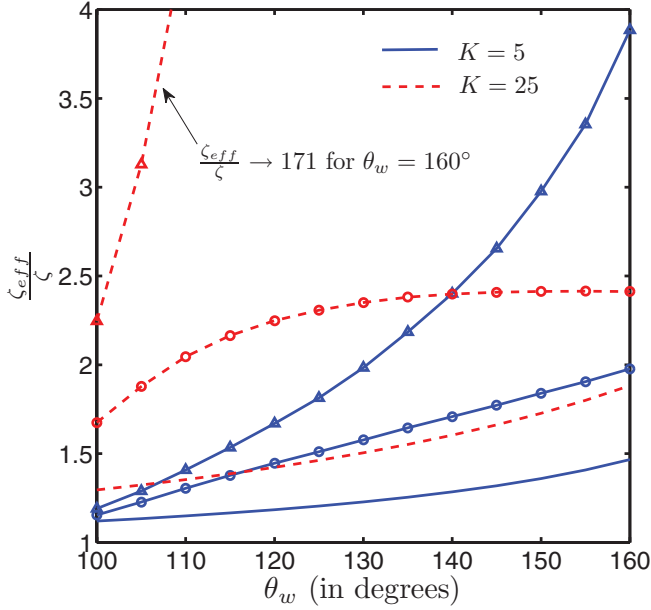


FIG. 4. (Color online) Variation of the effective normalized zeta potential with the contact angle for  $K = 5$  (represented by solid lines) and  $K = 25$  (represented by dashed lines) with  $\bar{\zeta} = -1$ ,  $\epsilon_{ratio} = 0.8$ , and  $\eta_{ratio} = 1/3$  kept constant. Results from the present approach are depicted by the plots without markers. For the two-layer approach, the slip-length-based route is depicted by  $\Delta$  while the direct bulk-velocity analogy route for the calculation of the effective zeta potential is depicted by  $\circ$ .

culminate in the form of massive electrokinetic pumping across the interfacial layer. In reality, however, this slip is only “apparent,” and the message of hydrophobic interactions at the wall gets propagated into the outer fluid through a continuously varying viscosity in tune with relative phase distributions consistent with the wall wettability. Interestingly, the discrepancies in the corresponding predictions do also sensitively depend on the relative magnitudes of the two length scales, namely, the interfacial thickness scale ( $\xi$ ) and the characteristic EDL length scale ( $\lambda_l$ ). Considering the value of  $C = (\frac{H}{\xi}) = 10$  (as adopted for the sets of simulation results presented in Fig. 4), two distinctive paradigms do manifest corresponding to the two values of the parameter  $K (= \frac{H}{\lambda_l})$  considered for plotting this figure. For  $K = 5$ ,  $\lambda_l > \xi$ , implicating that the near-wall velocity gradients are relatively weakly exaggerated through the use of a Navier slip boundary condition that may be somewhat inappropriate in carrying the sole burden of representing the wettability-electromechanical coupling at the interfacial layer. In addition, because of a relatively smaller interfacial thickness as compared to Debye length, consequences of variations in effective permittivity and viscosity across the interfacial layer do not turn out to be decisive in resulting in large deviations between the predictions from the two models, although the discrepancies do magnify as the contact angle at the wall is more progressively increased. On the other hand, for  $K = 25$ ,  $\lambda_l < \xi$ , implicating that property variations across the interfacial layer may turn out to be decisive towards predicting the net effective electrokinetic transport. This effect, aided by steep gradients of near-wall velocity that amplify the artifice of Navier slip condition at the

wall, exhibits a dramatic amplification in the predicted value of the zeta potential in the slip-based conceptual paradigm, as compared to the predictions from the present model.

## 2. Relative assessment of the two-layer route without slip-based considerations and the present approach

Can the discrepancy between the slip-based approach and the present approach be solely attributed to the slip-length-driven artifice of representing the interfacial hydrodynamics? Towards answering this question, we consider a third alternative approach, in which we invoke the discrete two-layer approach again, but calculate the effective zeta potential by considering the bulk transport directly, instead of going through a slip-based route. In other words, we intend to assess the predictions of the two-layer approach by considering the effective zeta potential prediction from the same bulk-velocity analogy route as that of the present approach. Interestingly, even in these circumstances (results from this third approach are shown in Figs. 3 and 4 with the aids of plots with circular markers) with a similar route of calculation of  $\zeta_{eff}$ , the two-layer model is seen to predict not only somewhat higher values of the normalized  $\zeta_{eff}$ , but may also exhibit contrasting qualitative trends as compared to those predicted by the present model (for instance, see the results corresponding to  $K = 25$ , as depicted in Fig. 4, in which the effective zeta potential, as predicted from the two-layer model, approaches an asymptote with the wall contact angle increasing beyond  $130^\circ$ ). This is quite unexpected, especially in cognizance of the fact that in addition to the adoption of the same route of determining the effective zeta potential, the two discrete layers are defined on the very same basis of the variation of the order parameter variable on which the present approach is based. Had it been only the quantitative mismatch, perhaps it could have been argued that the discrepancy was due to an erroneous representation of the interface, and corrections could be made through a fitting exercise. However, the qualitatively distinctive trends, effectively realized for thin EDLs, indicate that it must be the oversimplification of the actual physical variation of interfacial properties in terms of a discretized two-layer paradigm that is culpable for such discrepancies. It is important to mention in this context that the relative “thickness” of the EDL, in an effort to assess any such discrepancies, needs to be considered in relation to the thickness of the phase-changing interfacial layer, and not merely in comparison to the characteristic length scale of the confinement itself. Interesting cases, however, may arise when the confinement height itself becomes comparable to either of these two length scales. Such situations may involve the formation of a “thick” interfacial layer with overlapping EDLs; a paradigm falling clearly beyond the scope of the mathematical treatment outlined in this work.

## IV. SUMMARY AND CONCLUSIONS

In this study, we have illustrated some discrepancies in the traditional approaches of representing hydrophobicity-electrokinetics coupling through an effective interfacial slip. Our studies have revealed that the corresponding Navier slip boundary condition may artificially amplify the prediction of an augmented electrokinetic transport, as manifested through

an effective zeta potential. Our studies have further delineated that quantitative and even qualitative discrepancies in this regard do remain, even if the slip-based route is discarded and the effective zeta potential is predicted from the bulk transport characteristics realized through a discrete two-layer approach. As a remedial measure, we describe a phase-field-based approach in which the electrical permittivity and viscosity variations across the interfacial layer may be assessed in tune with the variations of a phase-field parameter that is allowed to evolve in accordance with a free-energy minimization principle. The distinctive feature of this approach compared to the two-layer approach, even if the depleted layer thickness in the later is estimated from the same phase-field paradigm, has been identified to rest on the fact that the two-layer approach effectively discretizes the phase transition across the interfacial layer in terms of transport phenomenon in two distinctive layers (a discrete layer of bulk liquid over a discrete depleted layer with homogeneous electrical and fluidic properties in the individual layers), whereas the present approach considers an explicit coupling of the interfacial phase fraction distribution with the electrostatic and fluidic transport across the interfacial layer by employing a thermodynamically consistent route. Our results do reveal that extreme care, indeed, needs to be taken while predicting “giant” augmentations in the effective zeta potential, and decisive assessment tests need to be conducted to rule out any model artifact that might potentially lead to such an elusive trend.

Practical implications of the outcome of the present study may be far reaching. As a specific example, one may cite the applications of miniaturized fluidic devices for energy harvesting. In such cases, predictions on the efficiency of energy conversion from hydraulic to electrical form, as realized through the considerations of establishment of a streaming potential, are sensitively dependent on the effective electrokinetic pumping as manifested through the effective zeta potential. Erroneous qualitative predictions in that regard, as well as fallacious quantitative trends with regard to gross overestimates in the concerned effective zeta potential values, may not only embed serious anomalies in the underlying design principle, but may also lead to prohibitively threatening malfunctioning of the devices thus conceptualized. Since the design principles of such devices are still traditionally based on the slip-based, two-layer paradigm, appropriate care needs to be taken in assessing their performance characteristics, and possibly a consistent thermodynamic route based on the phase-field formalism may be alternatively adopted to cater the specific design demands.

#### ACKNOWLEDGMENTS

J.C. and S.P. thank Debabrata DasGupta and Kaustav Chaudhury for useful discussions related to the phase-field modeling, and P. Kaushik for help in some preliminary numerical work during the initial stages.

#### APPENDIX A

In this Appendix, we briefly review a classical electrokinetic model, consistent with “slipping” hydrodynamics, and provide the mathematical details behind the derivation of the effective

zeta potential expressed in terms of the slip length. To capture the pertinent physics, one basically needs to solve the Navier-Stokes equations with electrokinetic body force terms, coupled with a Navier slip boundary condition at the wall. Description of the electrokinetic body force terms, in turn, depends on the potential distribution within the system. The potential distribution, again, is fundamentally related to the number densities of the ionic species. Therefore, it is necessary to mathematically describe the transport of the ionic species for obtaining their respective number densities, which may be achieved through the classical Nernst-Planck equation. Considering the presence of no interspecies interactions other than those between a particular diffusing species and the solvent [96], the same can be described as

$$\partial c_i / \partial t = -\nabla \cdot \mathbf{N}_i, \quad (\text{A1})$$

where  $\mathbf{N}_i$  is the net ionic flux and  $c_i$  is the local concentration of the  $i$ th ionic species. Considering a dilute solution limit,  $\mathbf{N}_i$  can be described as

$$\mathbf{N}_i = -D_i \left( \nabla c_i + \frac{z_i e}{k_B T} c_i \nabla \psi \right) + c_i \mathbf{u}, \quad (\text{A1a})$$

where  $D_i$  is the diffusivity,  $z_i$  is the ionic valence,  $e$  is the protonic charge,  $k_B$  is the Boltzmann constant,  $T$  is the absolute temperature,  $\psi$  is the potential due to the total electric field, and  $\mathbf{u}$  is the mass-averaged flow velocity. Substituting Eq. (A1a) into Eq. (A1), it follows that

$$\frac{\partial c_i}{\partial t} = D_i \nabla^2 c_i + D_i \frac{e z_i}{k_B T} \nabla \cdot (c_i \nabla \psi) - \nabla \cdot (c_i \mathbf{u}). \quad (\text{A2})$$

In order to resolve the potential field intrinsically coupled to this electrolyte species transport, one may refer to the Poisson equation:

$$\nabla \cdot (\epsilon \nabla \psi) = -\sum_j e z_j c_j, \quad (\text{A3})$$

where  $\epsilon$  is the permittivity of the solution and is, in general, not devoid of spatial gradients.

We now consider the model electro-osmotic problem as described in Sec. II A. With the considerations of identical homogeneous surface charging conditions of the walls within which the EOF is taking place and the fortunate orthogonality which does not disturb the equilibrium distribution, and assuming negligible contribution from the advection term, Eq. (A2) reduces to

$$\frac{\partial^2 c_{\pm}^0}{\partial y^2} = -\frac{z_{\pm} e}{k_B T} \frac{\partial}{\partial y} \left( c_{\pm}^0 \frac{\partial \psi^0}{\partial y} \right), \quad (\text{A4})$$

in the steady-state condition. Applying symmetry conditions at the channel center line, i.e.,  $\partial \psi^0(y=H)/\partial y = 0$  and  $\partial c_{\pm}^0(y=H)/\partial y = 0$  together with the approximation  $\psi^0(y=H) = 0$  and  $c_{\pm}^0(y=H) = 0$  under nonoverlapped EDL conditions, we obtain

$$c_{\pm}^0 = c^{\infty} \exp \left( -\frac{z_{\pm} e \psi^0}{k_B T} \right), \quad (\text{A5})$$

where  $c^{\infty}$  is the concentration in the electroneutral bulk. Equation (A5) is recognized to be the Boltzmann distribution, and may be combined with the Poisson equation Eq. (A3)

to obtain the celebrated Poisson-Boltzmann equation for the potential distribution screening the surface charge:

$$\frac{\partial}{\partial y} \left( \epsilon \frac{\partial \psi^0}{\partial y} \right) = -\rho_e \Rightarrow \frac{\partial}{\partial y} \left( \epsilon \frac{\partial \psi^0}{\partial y} \right) = \frac{1}{\lambda^2} \sinh \left( \frac{e z \psi^0}{k_B T} \right), \quad (\text{A6})$$

where  $\lambda = \sqrt{(\epsilon k_B T)/(2c^\infty e^2 z^2)}$ , using  $z = z_+ = -z_-$ .

In cases of electro-osmotic flows through narrow confinements, one typically resolves the solvent hydrodynamics through the Stokes equation (reduced form of the Navier-Stokes equation in the low Reynolds number regime) in a slightly modified form to incorporate additional forces due to osmotic pressure and electrical stresses. In a final simplified form, consistent with the considerations outlined above, the same reads (for details of the derivation and the underlying assumptions, see Ref. [107])

$$0 = \nabla \cdot (\eta \nabla \mathbf{u}) + \rho_e \mathbf{E}_{\text{app}}, \quad (\text{A7})$$

where  $\eta$  is the dynamic viscosity which, in general, may be a function of the spatial coordinates, and  $\mathbf{E}_{\text{app}}$  is an externally applied electrical field. Combining Eqs. (A6) and (A7), it follows that

$$0 = \frac{\partial}{\partial y} \left( \eta \frac{\partial u}{\partial y} \right) - \frac{\partial}{\partial y} \left( \epsilon \frac{\partial \psi}{\partial y} \right) E_{\text{app}}. \quad (\text{A8})$$

From this stage, we drop the superscript on  $\psi$ , with an understanding that it represents the quiescent condition potential that screens the surface charge.

Consistent with our objective, we solve Eq. (A8) subject to the following boundary conditions: First, a Navier slip boundary condition at the wall, through the specification of

a slip length  $b$ :

$$u|_{y=0} = b \left. \frac{\partial u}{\partial y} \right|_{y=0}, \quad (\text{A9})$$

and, second, the symmetry boundary condition at the channel center line:

$$\left. \frac{\partial u}{\partial y} \right|_{y=H} = 0. \quad (\text{A10})$$

Solution of Eq. (8), in conjunction with boundary conditions given by Eqs. (A9) and (A10), results in an expression of the velocity field:

$$u = \frac{\epsilon \psi E_{\text{app}}}{\eta} + b \frac{\epsilon E_{\text{app}}}{\eta} \left. \frac{\partial \psi}{\partial y} \right|_{y=0} - \frac{\epsilon E_{\text{app}}}{\eta} \psi \Big|_{y=0}. \quad (\text{A11})$$

The augmentation of flow velocities due to interfacial slip, as evident from Eq. (A11), is traditionally expressed in the electrokinetics literature through the introduction of an effective zeta potential,  $\zeta_{\text{eff}}$ . This is essentially defined by representing the bulk flow velocity in analogy with the Helmholtz-Smoluchowski velocity, so that  $u_{\text{bulk}} = -\eta \zeta_{\text{eff}} E_{\text{app}}/\eta$ . Considering the fact that [from Eq. (A11)]

$$u_{\text{bulk}} = u|_{y=H} = -\frac{\epsilon E_{\text{app}}}{\eta} \left[ \psi|_{y=0} + b \left( -\left. \frac{\partial \psi}{\partial y} \right|_{y=0} \right) \right], \quad (\text{A12})$$

and noting that  $\psi|_{y=H} = 0$  (in the absence of any EDL overlap), we obtain Eq. (1) mentioned in Sec. II A:

$$\zeta_{\text{eff}} = \zeta \left[ 1 + b \frac{\left( -\left. \frac{\partial \psi}{\partial y} \right|_{y=0} \right)}{\zeta} \right]. \quad (\text{A13})$$

- 
- [1] E. E. Meyer, K. J. Rosenberg, and J. Israelachvili, *Proc. Natl. Acad. Sci. USA* **103**, 15739 (2006).
- [2] B. J. Berne, J. D. Weeks, and R. Zhou, *Annu. Rev. Phys. Chem.* **60**, 85 (2009).
- [3] T. M. Squires and S. R. Quake, *Rev. Mod. Phys.* **77**, 977 (2005).
- [4] F. H. Stillinger, *J. Solution Chem.* **2**, 141 (1973).
- [5] C.-Y. Lee, A. McCammon, and P. J. Rossky, *J. Chem. Phys.* **80**, 4448 (1984).
- [6] K. Lum, D. Chandler, and J. D. Weeks, *J. Phys. Chem. B* **103**, 4570 (1999).
- [7] R. Steitz, T. Gutberlet, T. Hauss, B. Klosgen, R. Krastev, S. Schemmel, A. C. Simonsen, and G. H. Findenegg, *Langmuir* **19**, 2409 (2003).
- [8] D. Schwendel, T. Hayashi, R. Dahint, A. Pertsin, M. Grunze, R. Steitz, and F. Schreiber, *Langmuir* **19**, 2284 (2003).
- [9] D. A. Doshi, E. B. Watkins, J. N. Israelachvili, and J. Majewski, *Proc. Natl. Acad. Sci. USA* **102**, 9458 (2005).
- [10] M. Mezger, H. Reichert, S. Schoder, J. Okasinski, H. Schroder, H. Dosch, D. Palms, J. Ralston, and V. Honkimaki, *Proc. Natl. Acad. Sci. USA* **103**, 18401 (2006).
- [11] M. Maccarini, R. Steitz, M. Himmelhaus, J. Fick, S. Tatur, M. Wolff, M. Grunze, J. Janacek, and R. Netz, *Langmuir* **23**, 598 (2007).
- [12] J. Janacek and R. R. Netz, *Langmuir* **23**, 8417 (2007).
- [13] F. Sedlmeier, J. Janacek, C. Sendner, L. Bocquet, R. R. Netz, and D. Horinek, *Biointerphases* **3**, FC23 (2008).
- [14] M. Mezger, F. Selmeier, D. Horinek, H. Reichert, D. Pontoni, and H. Dosch, *J. Am. Chem. Soc.* **132**, 6735 (2010).
- [15] S. Chattopadhyay, A. Uysal, B. Stripe, Y. G. Ha, T. J. Marks, E. A. Karapetrova, and P. Dutta, *Phys. Rev. Lett.* **105**, 037803 (2010).
- [16] M. Walz, S. Gerth, P. Falus, M. Klimczak, T. H. Metzger, and A. Magerl, *J. Phys.: Condens. Matter* **23**, 324102 (2011).
- [17] J. Israelachvili, *Intermolecular and Surface Forces* (Academic, Amsterdam, 2003).
- [18] E. Ruckenstein and P. Rajora, *J. Colloid Interface Sci.* **96**, 488 (1983).
- [19] N. V. Churaev, V. D. Sobolev, and A. Somov, *J. Colloid Interface Sci.* **97**, 574 (1984).
- [20] O. I. Vinogradova, *Langmuir* **11**, 2213 (1995).
- [21] O. I. Vinogradova, *Int. J. Miner. Process.* **56**, 31 (1999).
- [22] J.-L. Barrat and L. Bocquet, *Phys. Rev. Lett.* **82**, 4671 (1999).
- [23] Y. Zhu and S. Granick, *Phys. Rev. Lett.* **87**, 096105 (2001).
- [24] P. G. de Gennes, *Langmuir* **18**, 3413 (2002).
- [25] D. Andrienko, B. Dünweg, and O. I. Vinogradova, *J. Chem. Phys.* **119**, 13106 (2003).

- [26] D. C. Tretheway and C. D. Meinhart, *Phys. Fluids* **16**, 1509 (2004).
- [27] C. Cottin-Bizonne, J.-L. Barrat, L. Bocquet, and E. Charlaix, *Nat. Mater.* **2**, 237 (2003).
- [28] M. Sbragaglia, R. Benzi, L. Biferale, S. Succi, and F. Toschi, *Phys. Rev. Lett.* **97**, 204503 (2006).
- [29] S. Chakraborty, *Phys. Rev. Lett.* **99**, 094504 (2007).
- [30] K. Watanabe, Y. Udagawa, and H. Udagawa, *J. Fluid Mech.* **381**, 225 (1999).
- [31] R. Pit, H. Hervet, and L. Léger, *Phys. Rev. Lett.* **85**, 980 (2000).
- [32] V. S. J. Craig, C. Neto, and D. R. M. Williams, *Phys. Rev. Lett.* **87**, 054504 (2001).
- [33] J. Baudry, E. Charlaix, A. Tonck, and D. Mazuyer, *Langmuir* **17**, 5232 (2001).
- [34] J.-T. Cheng and N. Giordano, *Phys. Rev. E* **65**, 031206 (2002).
- [35] C. Cottin-Bizonne, S. Jurine, J. Baudry, J. Crassous, F. Restagno, and E. Charlaix, *Eur. Phys. J. E* **9**, 47 (2002).
- [36] D. C. Tretheway and C. D. Meinhart, *Phys. Fluids* **14**, L9 (2002).
- [37] C.-H. Choi, K. J. A. Westin, and K. S. Breuer, *Phys. Fluids* **15**, 2897 (2003).
- [38] J.-H. J. Cho, B. M. Law, and F. Rieutord, *Phys. Rev. Lett.* **92**, 166102 (2004).
- [39] C. Neto, D. R. Evans, E. Bonaccorso, H.-J. Butt, and V. S. J. Craig, *Rep. Prog. Phys.* **68**, 2859 (2005).
- [40] T. Schmatko, H. Hervet, and L. Leger, *Phys. Rev. Lett.* **94**, 244501 (2005).
- [41] C. Cottin-Bizonne, B. Cross, A. Steinberger, and E. Charlaix, *Phys. Rev. Lett.* **94**, 056102 (2005).
- [42] P. Joseph and P. Tabeling, *Phys. Rev. E* **71**, 035303 (2005).
- [43] P. Huang and K. S. Breuer, *Phys. Fluids* **19**, 028104 (2007).
- [44] G. R. Willmott and J. L. Tallon, *Phys. Rev. E* **76**, 066306 (2007).
- [45] C. Bouzigues, L. Bocquet, E. Charlaix, C. Cottin-Bizonne, B. Cross, L. Joly, A. Steinberger, C. Ybert, and P. Tabeling, *Philos. Trans. R. Soc., A* **366**, 1455 (2008).
- [46] A. Maali, T. Cohen-Bouhacina, and H. Kellay, *Appl. Phys. Lett.* **92**, 053101 (2008).
- [47] A. Maali and B. Bhushan, *J. Phys.: Condens. Matter* **20**, 315201 (2008).
- [48] U. Ulmanella and C.-M. Ho, *Phys. Fluids* **20**, 101512 (2008).
- [49] C. I. Bouzigues, P. Tabeling, and L. Bocquet, *Phys. Rev. Lett.* **101**, 114503 (2008).
- [50] C. L. Henry and V. S. J. Craig, *PhysChemChemPhys* **11**, 9514 (2009).
- [51] Y. Wang, B. Bhushan, and A. Maali, *J. Vac. Sci. Technol. A* **27**, 754 (2009).
- [52] B. Bhushan, Y. Wang, and A. Maali, *Langmuir* **25**, 8117 (2009).
- [53] O. I. Vinogradova, K. Koynov, A. Best, and F. Feuillebois, *Phys. Rev. Lett.* **102**, 118302 (2009).
- [54] S. Yordanov, A. Best, H.-J. Butt, and K. Koynov, *Opt. Express* **17**, 21149 (2009).
- [55] S. P. McBride and B. M. Law, *Phys. Rev. E* **80**, 060601 (2009).
- [56] Y. Wang and B. Bhushan, *Soft Matter* **6**, 29 (2010).
- [57] H. Li and M. Yoda, *J. Fluid Mech.* **662**, 269 (2010).
- [58] M.-C. Audry, A. Piednoir, P. Joseph, and E. Charlaix, *Faraday Discuss.* **146**, 113 (2010).
- [59] L. Zhu, P. Attard, and C. Neto, *Langmuir* **27**, 6712 (2011).
- [60] J. Koplik, J. R. Banavar, and J. F. Willemsen, *Phys. Fluids A* **1**, 781 (1989).
- [61] P. A. Thompson and M. O. Robbins, *Phys. Rev. A* **41**, 6830 (1990).
- [62] P. A. Thomson and S. M. Troian, *Nature (London)* **389**, 360 (1997).
- [63] J.-L. Barrat and L. Bocquet, *Faraday Discuss.* **112**, 119 (1999).
- [64] M. Cieplak, J. Koplik, and J. R. Banavar, *Phys. Rev. Lett.* **86**, 803 (2001).
- [65] V. P. Sokhan, D. Nicholson, and N. Quirke, *J. Chem. Phys.* **115**, 3878 (2001).
- [66] L. Joly, C. Ybert, E. Trizac, and L. Bocquet, *Phys. Rev. Lett.* **93**, 257805 (2004).
- [67] L. Joly, C. Ybert, E. Trizac, and L. Bocquet, *J. Chem. Phys.* **125**, 204716 (2006).
- [68] R. S. Voronov, D. V. Papavassiliou, and L. L. Lee, *J. Chem. Phys.* **124**, 204701 (2006).
- [69] N. V. Priezjev, *Phys. Rev. E* **75**, 051605 (2007).
- [70] A. Niavarani and N. V. Priezjev, *Phys. Rev. E* **77**, 041606 (2008).
- [71] A. Martini, H.-Y. Hsu, N. A. Patankar, and S. Lichter, *Phys. Rev. Lett.* **100**, 206001 (2008).
- [72] V. P. Sokhan and N. Quirke, *Phys. Rev. E* **78**, 015301 (2008).
- [73] D. M. Huang, C. Sendner, D. Horinek, R. R. Netz, and L. Bocquet, *Phys. Rev. Lett.* **101**, 226101 (2008).
- [74] C. Sendner, D. Horinek, L. Bocquet, and R. R. Netz, *Langmuir* **25**, 10768 (2009).
- [75] N. V. Priezjev, *Phys. Rev. E* **82**, 051603 (2010).
- [76] X. Yang and Z. C. Zheng, *ASME J. Fluids Eng.* **132**, 061201 (2010).
- [77] A. Alizadeh Pahlavan and J. B. Freund, *Phys. Rev. E* **83**, 021602 (2011).
- [78] H. Zhang, Z. Zhang, and H. Ye, *Microfluid. Nanofluid.* **12**, 107 (2012).
- [79] J. S. Hansen, B. D. Todd, and P. J. Davis, *Phys. Rev. E* **84**, 016313 (2011).
- [80] M. D. Ma, L. Shen, J. Sheridan, J. Z. Liu, C. Chen, and Q. Zheng, *Phys. Rev. E* **83**, 036316 (2011).
- [81] L. Zhu, D. Tretheway, L. Petzold, and C. Meinhart, *J. Comput. Phys.* **202**, 181 (2005).
- [82] R. Benzi, L. Biferale, M. Sbragaglia, S. Succi, and F. Toschi, *Europhys. Lett.* **74**, 651 (2006).
- [83] R. Benzi, L. Biferale, M. Sbragaglia, S. Succi, and F. Toschi, *Phys. Rev. E* **74**, 021509 (2006).
- [84] J. Harting, C. Kunert, and H. J. Herrmann, *Europhys. Lett.* **75**, 328 (2006).
- [85] N. K. Ahmed and M. Hecht, *J. Stat. Mech.: Theory Exp.* (2009) P09017.
- [86] J. Zhang, *Microfluid. Nanofluid.* **10**, 1 (2011); Sec. 5.3 is of particular relevance.
- [87] S. Chakraborty, *Phys. Rev. Lett.* **100**, 097801 (2008).
- [88] T. Biben and L. Joly, *Phys. Rev. Lett.* **100**, 186103 (2008).
- [89] W. Mickel, L. Joly, and T. Biben, *J. Chem. Phys.* **134**, 094105 (2011).
- [90] E. Lauga, M. Brenner, and H. Stone, in *Springer Handbook of Experimental Fluid Mechanics*, edited by C. Tropea, A. L. Yarin, and J. F. Foss (Springer, Berlin, 2007), pp. 1219–1240.
- [91] L. Bocquet and J.-L. Barrat, *Soft Matter* **3**, 685 (2007).
- [92] J. Eijkel, *Lab Chip* **7**, 299 (2007).
- [93] L. Bocquet and E. Charlaix, *Chem. Soc. Rev.* **39**, 1073 (2010).
- [94] O. I. Vinogradova and A. V. Belyaev, *J. Phys.: Condens. Matter* **23**, 184104 (2011).

- [95] R. J. Hunter, *Zeta Potential in Colloid Science* (Academic Press, London, 1981).
- [96] J. Newman and K. E. Thomas-Alyea, *Electrochemical Systems*, 3rd ed. (Wiley-Interscience, Hoboken, NJ, 2004).
- [97] V. M. Muller, I. P. Sergeeva, V. D. Sobolev, and N. V. Churaev, *Colloid J. USSR* **48**, 606 (1986).
- [98] J. Yang and D. Y. Kwok, *Langmuir* **19**, 1047 (2003).
- [99] J. Yang and D. Y. Kwok, *Anal. Chim. Acta* **507**, 39 (2004).
- [100] A. Ajdari and L. Bocquet, *Phys. Rev. Lett.* **96**, 186102 (2006).
- [101] L. Joly, C. Ybert, E. Trizac, and L. Bocquet, *J. Chem. Phys.* **125**, 204716 (2006).
- [102] D. M. Huang, C. Cottin-Bizonne, C. Ybert, and L. Bocquet, *Phys. Rev. Lett.* **101**, 064503 (2008).
- [103] T. M. Squires, *Phys. Fluids* **20**, 092105 (2008).
- [104] V. Tandon and B. J. Kirby, *Electrophoresis* **29**, 1102 (2008).
- [105] A. V. Belyaev and O. I. Vinogradova, *Phys. Rev. Lett.* **107**, 098301 (2011).
- [106] P. Goswami and S. Chakraborty, *Microfluid. Nanofluid.* **11**, 255 (2011).
- [107] R. F. Probstein, *Physicochemical Hydrodynamics*, 2nd ed. (Wiley-Interscience, Hoboken, NJ, 2003).
- [108] J. W. Cahn, *J. Chem. Phys.* **66**, 3667 (1977).
- [109] V. E. Badalassi, H. D. Ceniceros, and S. Banerjee, *J. Comput. Phys.* **190**, 371 (2003).
- [110] D. Jasnow and D. Viñals, *Phys. Fluids* **8**, 660 (1996).
- [111] D. Jacqmin, *J. Comput. Phys.* **155**, 96 (1999).
- [112] O. Kuksenok and A. C. Balazs, *Phys. Rev. E* **68**, 011502 (2003).
- [113] O. Kuksenok, D. Jasnow, and A. C. Balazs, *Phys. Rev. E* **68**, 051505 (2003).
- [114] O. Kuksenok, D. Jasnow, and A. C. Balazs, *Phys. Rev. Lett.* **95**, 240603 (2005).
- [115] P. Yue, J. J. Feng, C. Liu, and J. Shen, *J. Fluid Mech.* **515**, 293 (2004).
- [116] V. V. Khataevkar, P. D. Anderson, and H. E. H. Meijer, *J. Fluid Mech.* **572**, 367 (2007).
- [117] O. A. Folovskaya, A. A. Nepomnyashchy, A. Oron, and A. A. Golovin, *Phys. Fluids* **20**, 112105 (2008).
- [118] U. Thiele, S. Madruga, and L. Frastia, *Phys. Fluids* **19**, 122106 (2007).
- [119] S. Madruga and U. Thiele, *Phys. Fluids* **21**, 062104 (2009).
- [120] S. Madruga and U. Thiele, *Eur. Phys. J.: Special Topics* **192**, 101 (2011).
- [121] L.-Q. Chen, *Annu. Rev. Mater. Res.* **32**, 113 (2002).
- [122] S. R. de Groot and P. Mazur, *Non-equilibrium Thermodynamics* (North Holland, Amsterdam, 1962).
- [123] D. Bonn and D. Ross, *Rep. Prog. Phys.* **64**, 1085 (2001).
- [124] L. M. Pismen and Y. Pomeau, *Phys. Rev. E* **62**, 2480 (2000).
- [125] A. H. Nayfeh, *Introduction to Perturbation Techniques* (Wiley-VCH, New York, 1993).
- [126] R. J. LeVeque, *Finite Difference Methods of Ordinary and Partial Differential Equations* (SIAM, Philadelphia, PA, 2007).
- [127] H. Ding and P. D. M. Spelt, *Phys. Rev. E* **75**, 046708 (2007).
- [128] R. Borcia and M. Bestehorn, *Eur. Phys. J. B* **44**, 101 (2005).
- [129] J. Park, X.-Q. Feng, and W. Lu, *J. Appl. Phys.* **109**, 034309 (2011).
- [130] G. Le and J. Zhang, *Langmuir* **27**, 5366 (2011).
- [131] N. Mishchuk, *J. Colloid Interface Sci.* **320**, 599 (2008).
- [132] N. Mishchuk, *Adv. Colloid Interface Sci.* **168**, 149 (2011).
- [133] S. V. Patankar, *Numerical Heat Transfer and Fluid Flow* (Taylor & Francis, Kundli, 2004).